Liquid Crystals
Publication details, including instructions for authors and subscription information:
http://www.informaworld.com/smpp/title~content=t713926090

Influence of ionic transport on deformations of homeotropic nematic layers with positive flexoelectric coefficients

Mariola Buczkowska[a]; Grzegorz Derfel[a]
[a] Institute of Physics, Technical University of Łódź, 93-005 Łódź, Poland

To cite this Article Buczkowska, Mariola and Derfel, Grzegorz(2005) 'Influence of ionic transport on deformations of homeotropic nematic layers with positive flexoelectric coefficients', Liquid Crystals, 32: 10, 1285 — 1293
To link to this Article: DOI: 10.1080/02678290500303221
URL: http://dx.doi.org/10.1080/02678290500303221

Liquid Crystals, Vol. 32, No. 10, October 2005, 1285–1293

Influence of ionic transport on deformations of homeotropic nematic layers with positive flexoelectric coefficients

MARIOLA BUCZKOWSKA* and GRZEGORZ DERFEL
Institute of Physics, Technical University of Łódź, ul. Wólczańska 219, 93-005 Łódź, Poland

(*Received 19 April 2005; accepted 21 June 2005*)

Electric field-induced deformations of homeotropic nematic liquid crystal layers were studied numerically. A positive sum of the flexoelectric coefficients and a small negative dielectric anisotropy of the nematic material were adopted. Finite surface anchoring strength was assumed. The flow of ionic current was taken into account, the weak electrolyte model being used for description of the electric properties. The director orientation, the electric potential and the ion concentrations were calculated as functions of the coordinate normal to the layer. Calculations show that the threshold for deformation depends on the distributions of the ions (which are influenced by their mobilities), by the ion generation constant and by the properties of the electrodes. When the electrodes have pronounced blocking character and the ion concentration is large, a high and non-uniform electric field is created by the subelectrode ion space charges. This causes drastic decrease of the threshold voltage, much below the value U_f valid for an insulating nematic. At moderate concentrations, the electric field gradient arises in the bulk due to the difference between the mobilities of positive and negative ions. It favours deformation, therefore the threshold is reduced below U_f. When the electrodes are well conducting, there are no significant space charges and the threshold voltage remains close to U_f. The same value occurs when the space charges are negligible at very low ion contents.

1. Introduction

Electric field-induced deformations of nematic layers arise as a result of torques exerted on the director in the bulk of the layer as well as at the surfaces [1]. These torques are due to the dielectric anisotropy and flexoelectric properties of the nematic. The flexoelectric deformations depend on the subsurface electric field strength which induces the surface torque, and on the electric field gradient which is responsible for the torque in the bulk. The dielectric torque is due to the electric field in the bulk. When the boundary plates play the role of electrodes, and the surface alignment is strictly planar or homeotropic, deformations arise above some threshold voltage. The form of the deformation results from the relationship between the magnitudes and signs of flexoelectric torques as well as from the magnitude and sign of the dielectric torque; it is also restricted by torques due to surface anchoring interactions. Therefore all the effects which influence the electric field distribution in the layer are significant. The ion space charge redistributed under the action of an external voltage is the most important. One may suppose that the distribution of the space charge is affected by the transport properties of the system, i.e. by the processes of generation and recombination of the ions, their mobilities and diffusion coefficients and by the rate of electrode processes.

In previous papers [2, 3] we showed numerically that under the assumption of perfectly blocking electrodes the threshold voltage depends not only on the sum of the flexoelectric coefficients $e_{11}+e_{33}$, dielectric anisotropy $\Delta\varepsilon$ and surface anchoring strength W, but also on the concentration N_0 of the ions which are usually present in the liquid crystal material. It may be significantly decreased if the flexoelectric properties are sufficiently strong, the surface anchoring sufficiently weak, and the ion concentration sufficiently high.

In this paper we present the results of calculations concerning the homeotropic layer of a weakly anchored nematic with a positive sum of the flexoelectric coefficients and negative dielectric anisotropy. The flow of ionic current was taken into account, and the electric properties described in terms of the weak electrolyte model [4]. A simple model for the electrode contacts was used, allowing us to consider various rates of electrode processes that determine the current flow across the layer.

*Corresponding author. Email: mbuczkow@p.lodz.pl

Liquid Crystals
ISSN 0267-8292 print/ISSN 1366-5855 online © 2005 Taylor & Francis
http://www.tandf.co.uk/journals
DOI: 10.1080/02678290500303221

The results show that the threshold voltage is affected by the properties of the nematic–electrode contacts. The flow of current influences the ionic space charge distribution and the electric field distribution and therefore the dielectric and flexoelectric torques. In consequence, the decrease of the threshold voltage occurs at moderate ion concentrations if the electrodes are poorly conducting. This reduction is attributed to the electric field gradient in the bulk which is a consequence of the unequal mobilities $\mu^{\pm}$ (and diffusion coefficients $D^{\pm}$) of positive and negative ions. (It is commonly accepted that $\mu^{-} \gg \mu^{+}$ [5, 6].) The resulting asymmetry of the electric field distribution gives rise to the prevailing torque, which in the case of $e_{11}+e_{33}>0$ favours deformation. Additional calculations show that for $\mu^{-}=\mu^{+}$ the reduction of the threshold is much weaker. When the electrodes are strongly blocking and the ion concentration is high, the threshold is also reduced, but this effect is due to the large subsurface electric field which induces a strong destabilizing surface torque of flexoelectric nature. (Analogous calculations performed for negative flexoelectric coefficients, $e_{11}+e_{33}<0$, which yielded opposite effects to some extent, are the subject of a separate paper [7].)

In the next section, the parameters of the system under consideration and the basic equations are given. In § 3, the results of calculations are presented; these are discussed in § 4.

2. Method

2.1. *Geometry and parameters*

The nematic liquid crystal was confined between two infinite plates which played the role of electrodes and were parallel to the xy-plane and positioned at $z=\pm d/2$. A voltage U was applied between them. The lower electrode ($z=-d/2$) was earthed. The director $\mathbf{n}$ was parallel to the xz-plane; its orientation described by the angle $\theta(z)$, measured between $\mathbf{n}$ and the z-axis. The material and layer parameters were the same as in our previous paper [2], with the exception that the sum of the flexoelectric coefficients is positive here, i.e. $e_{11}+e_{33}=40\,\mathrm{pC\,m^{-1}}$. They are briefly listed as follows: thickness $d=20\,\mu\mathrm{m}$, homeotropic alignment, anchoring strength $W=2\times10^{-5}\,\mathrm{J\,m^{-2}}$, elastic constants $k_{11}=6.2\times10^{-12}\,\mathrm{N}$ and $k_{33}=8.6\times10^{-12}\,\mathrm{N}$, the dielectric constant components $\varepsilon_{\parallel}=4.7$ and $\varepsilon_{\perp}=5.4$.

The average ion concentration N_{av} is defined as

$$N_{\mathrm{av}}=\frac{1}{2d}\left\{\int_{-d/2}^{d/2}[N^{+}(z)+N^{-}(z)]\mathrm{d}z\right\} \qquad (1)$$

where $N^{\pm}(z)$ denote the concentrations of ions of corresponding sign, ranging from 10^{17} to $3\times10^{20}\,\mathrm{m^{-3}}$. The transport of the ions was characterized by typical values of mobility coefficients $\mu_{\parallel}{}^{-}=1.5\times10^{-9}\,\mathrm{m^2\,V^{-1}\,s^{-1}}$, $\mu_{\perp}{}^{-}=1\times10^{-9}\,\mathrm{m^2\,V^{-1}\,s^{-1}}$, $\mu_{\parallel}{}^{+}=1.5\times10^{-10}\,\mathrm{m^2\,V^{-1}\,s^{-1}}$, $\mu_{\perp}{}^{+}=1\times10^{-10}\,\mathrm{m^2\,V^{-1}\,s^{-1}}$ [8, 9], and diffusion coefficients $D^{\pm}_{\parallel,\perp}=(k_{\mathrm{B}}T/q)\mu^{\pm}_{\parallel,\perp}$ where q is the absolute value of the ionic charge, k_{B} is the Boltzmann constant and T is the absolute temperature. We have also performed additional calculations for two values of equal mobilities (preserving the ratio $\mu_{\parallel}{}^{\pm}/\mu_{\perp}{}^{\pm}=1.5$): $\mu_{\perp}{}^{+}=\mu_{\perp}{}^{-}=1\times10^{-9}\,\mathrm{m^2\,V^{-1}\,s^{-1}}$, and $\mu_{\perp}{}^{+}=\mu_{\perp}{}^{-}=1\times10^{-10}\,\mathrm{m^2\,V^{-1}\,s^{-1}}$.

The weak electrolyte model [4] was adopted for the description of electrical phenomena in the layer. The ion concentration was determined by the generation and recombination constants. The generation constant β depended on the electric field strength E [10]: $\beta=\beta_0\left(1+\frac{q^3}{8\pi\varepsilon_0\overline{\varepsilon}k_{\mathrm{B}}^2T^2}E\right)$, where $\overline{\varepsilon}=\left(2\varepsilon_{\perp}+\varepsilon_{\parallel}\right)/3$. Its value in the absence of the field, β_0, was varied from 10^{17} to $10^{23}\,\mathrm{m^{-3}\,s^{-1}}$ in order to control the ion concentration. The recombination constant was calculated from the formula $\alpha=\frac{2q\overline{\mu}}{\varepsilon_0\overline{\varepsilon}}$ [10], where $\overline{\mu}=\left[\left(2\mu_{\perp}^{+}+\mu_{\parallel}^{+}\right)/3+\left(2\mu_{\perp}^{-}+\mu_{\parallel}^{-}\right)/3\right]/2$. It was equal to $4.5\times10^{-18}\,\mathrm{m^3\,s^{-1}}$ in the case of $\mu^{-}\gg\mu^{+}$, and to 8.2×10^{-18} and $8.2\times10^{-19}\,\mathrm{m^3\,s^{-1}}$ when the equal mobilities were of order 10^{-9} and $10^{-10}\,\mathrm{m^2\,V^{-1}\,s^{-1}}$, respectively.

The transport of ions in the bulk is governed by two equations of continuity for ions of both signs:

$$d(\beta-\alpha N^{+}N^{-})=\frac{\mathrm{d}J_z^{\pm}}{\mathrm{d}\zeta} \qquad (2)$$

where $J_z^{\pm}=\mp\frac{1}{d}\left(\mu_{zz}^{\pm}N^{\pm}\frac{\mathrm{d}V}{\mathrm{d}\zeta}\pm D_{zz}^{\pm}\frac{\mathrm{d}N^{\pm}}{\mathrm{d}\zeta}\right)$ denotes the flux of ions of given sign, i.e. the number of ions which pass through a surface $\zeta=const$, counted per unit area and per unit time. The z-components of mobility and diffusion coefficients are given by $\mu_{zz}^{\pm}=\mu_{\perp}^{\pm}+\Delta\mu^{\pm}\cos^2\theta$ and $D_{zz}^{\pm}=D_{\perp}^{\pm}+\Delta D^{\pm}\cos^2\theta$, respectively, where $\Delta\mu^{\pm}=\mu_{\parallel}^{\pm}-\mu_{\perp}^{\pm}$ and $\Delta D^{\pm}=D_{\parallel}^{\pm}-D_{\perp}^{\pm}$ denote the anisotropies of each quantity.

The conducting properties of the layer are characterized by coefficient K_{r} which determines the rate of the electrode processes.

According to our model, the flux of ions of given sign which approach a chosen electrode (or move away from it) is equal to the net change in the number of ions resulting from the generation and neutralization processes at the electrode per unit area and per unit time. The speed of neutralization of the ions, $n_{\mathrm{r}}^{\pm}$, is proportional to their concentration: $n_{\mathrm{r}}^{\pm}=K_{\mathrm{r}}^{\pm}N^{\pm}$; and

the speed of generation, $n_g^{\pm}$, is proportional to the concentration N_d of the neutral dissociable molecules: $n_g^{\pm} = K_g^{\pm} N_d$, where $K_r^{\pm}$ and $K_g^{\pm} = K_r^{\pm} N_0 / N_d$ are suitable constants of proportionality and $N_0 = (\beta_0/\alpha)^{\frac{1}{2}}$.

The rates of generation and neutralization of the ions at the electrodes can be interpreted in terms of a model in which they are determined by the activation energies φ of corresponding electrochemical reactions. For example, the rate of neutralization of the negative ion, occurring by the transfer of an electron from the ion to the electrode, amounts to $K_r = k_r \exp(-\varphi/k_B T)$, where k_r is a constant. A similar formula can be used for the generation constant of positive ions occurring by the transfer of an electron from a neutral molecule to the electrode. (In general, the energy barriers φ can be of different height for every electrode process.) The energy barrier is affected by the electric field existing at the electrode, i.e. increased or decreased by $\Delta\varphi = EqL$, where L is the thickness of the subelectrode region, of the order of several molecular lengths. In our calculations $L = 10\,\text{nm}$.

As a result of the above assumptions, the boundary conditions take the forms:

$$\mp \mu_{zz}^{\pm} N^{\pm} \frac{dV}{d\zeta} - D_{zz}^{\pm} \frac{dN^{\pm}}{d\zeta} = \left[-N^{\pm} K_r \exp\left(\pm \Delta\varphi / k_B T\right) + N_0 K_r \exp\left(\mp \Delta\varphi / k_B T\right) \right] d \quad \text{for } \zeta = -1/2 \tag{3}$$

$$\mp \mu_{zz}^{\pm} N^{\pm} \frac{dV}{d\zeta} - D_{zz}^{\pm} \frac{dN^{\pm}}{d\zeta} = \left[-N^{\pm} K_r \exp\left(\mp \Delta\varphi / k_B T\right) + N_0 K_r \exp\left(\pm \Delta\varphi / k_B T\right) \right] d \quad \text{for } \zeta = +1/2 \tag{4}$$

The left hand sides of these equations represent the fluxes of the ions at the electrodes. The first terms on the right hand sides denote the numbers of ions which are neutralized, and the second terms denote the numbers of ions generated at the electrodes in the course of accepting or donating the electrons by the neutral molecules.

In order to illustrate possible essentially distinct behaviours of the layer, the calculations were carried out with several different values of K_r: 10^{-7}, 10^{-6}, 10^{-5}, 10^{-4} and $10^{-3}\,\text{ms}^{-1}$, whereas N_d was equal to $10^{24}\,\text{m}^{-3}$ in every case.

2.2. *Basic equations*

The problem is considered to be one-dimensional. The reduced co-ordinate, $\zeta = z/d$, is used in the following. The functions $\theta(\zeta)$ and $V(\zeta)$, which describe the director orientation and the potential distribution within the layer, are determined by the torque equation:

$$\frac{1}{2}(k_b - 1)\sin 2\theta \left(\frac{d\theta}{d\zeta}\right)^2 - \left(\sin^2\theta + k_b \cos^2\theta\right)\frac{d^2\theta}{d\zeta^2} + \frac{1}{2}\frac{\varepsilon_0 \Delta\varepsilon}{k_{11}} \sin 2\theta \left(\frac{dV}{d\zeta}\right)^2 + \frac{1}{2}\frac{e_{11} + e_{33}}{k_{11}} \sin 2\theta \left(\frac{d^2V}{d\zeta^2}\right) = 0 \tag{5}$$

and the electrostatic equation:

$$\rho(\zeta) d^2 + \varepsilon_0 \left(\varepsilon_\perp + \Delta\varepsilon \cos^2\theta\right)\frac{d^2V}{d\zeta^2} - \varepsilon_0 \Delta\varepsilon \sin 2\theta \frac{dV}{d\zeta}\frac{d\theta}{d\zeta} + (e_{11} + e_{33})\cos 2\theta \left(\frac{d\theta}{d\zeta}\right)^2 + \frac{1}{2}(e_{11} + e_{33})\sin 2\theta \frac{d^2\theta}{d\zeta^2} = 0 \tag{6}$$

where $k_b = k_{33}/k_{11}$ and $\rho(\zeta) = q[N^+(\zeta) - N^-(\zeta)]$ is the space charge density.

The boundary conditions for $\theta(\zeta)$ are determined by the equations

$$\pm \left[\frac{1}{2}\frac{e_{11} + e_{33}}{k_{11}} \sin 2\theta(\pm 1/2) \frac{dV}{d\zeta}\bigg|_{\pm 1/2} - \left(\sin^2\theta(\pm 1/2) + k_b \cos^2\theta(\pm 1/2)\right)\frac{d\theta}{d\zeta}\bigg|_{\pm 1/2} \right] - \frac{1}{2}\gamma \sin 2\theta(\pm 1/2) = 0 \tag{7}$$

for $\zeta = \pm 1/2$, where $\gamma = Wd/k_{11}$. The boundary conditions for the potential are $V(-1/2) = 0$ and $V(1/2) = U$.

The set of ten equations (2)–(7) was solved numerically. The nematic layer was divided into $M = 858$ sublayers described by the discrete variables θ_i, V_i, N_i^+ and N_i^-. The differential equations (2)–(7) were replaced by difference equations. The Gauss–Seidel method was applied for solution of algebraic equations resulting from equations (5)–(7). The two sets of equations obtained from (2)–(4) for positive and negative ions were described by tridiagonal matrices and were solved by means of the sweep method [11]. The computed θ_i, V_i, N_i^+ and N_i^- values approximate the corresponding functions of the reduced coordinate ζ. The director configurations, described by the angle $\theta(\zeta)$, the electric potential distributions $V(\zeta)$ and the ion

concentrations $N^{\pm}(\zeta)$ were calculated for various voltages and generation constants β_0. The results allowed determination of the threshold voltages U_T for the deformations.

3. Results

Six sets of solutions $\theta(\zeta)$, $|E|(\zeta)$ and $N^{\pm}(\zeta)$ are chosen to illustrate the essential results of the computations. In the following, they are denoted by numbers from 1 to 6. The corresponding average ion concentrations N_{av} (in m^{-3}), rate of the electrode processes K_r (in ms^{-1}), and voltages U (in volts) are as follows. 1: $N_{av}=2.6\times10^{18}$, $K_r=10^{-3}$, $U=3.38$; 2: $N_{av}=4.0\times10^{16}$, $K_r=10^{-6}$, $U=3.58$; 3: $N_{av}=8.9\times10^{18}$, $K_r=10^{-7}$, $U=1.13$; 4: $N_{av}=2.6\times10^{18}$, $K_r=10^{-4}$, $U=1.88$; 5: $N_{av}=1.3\times10^{20}$, $K_r=10^{-7}$, $U=0.67$; 6: $N_{av}=4.9\times10^{20}$, $K_r=10^{-5}$, $U=3.37$.

3.1. *Threshold voltage*

All the deformations of the considered layer have threshold character. For given elastic constants, dielectric anisotropy, flexoelectric properties and surface anchoring, the threshold voltage is influenced by the ion distributions which depend on the generation constant β_0, as well as on the properties of the electrodes. This influence is illustrated in figure 1, where the threshold voltage U_T is plotted as a function of average ion concentration N_{av} for five values of K_r.

For very low average concentration ($N_{av}<10^{17}\,m^{-3}$) and independently of the properties of the electrodes, the threshold is quite close to the theoretical value $U_f=3.53$ V predicted for perfectly insulating nematics by the formula

$$\cot\left(\pi\frac{U_f}{U_c}\right)=\frac{Wd}{2\pi k_{33}}\frac{U_c}{U_f}\left\{\left(\frac{\pi k_{33}}{Wd}\frac{U_f}{U_c}\right)^2\left[\left(\frac{U_c(e_{11}+e_{33})}{\pi k_{33}}\right)^2+1\right]-1\right\} \quad (8)$$

where $U_c=\pi\left(\frac{k_{33}}{\varepsilon_0|\Delta\varepsilon|}\right)^{\frac{1}{2}}$ [12]. The interesting differences between values obtained for various electrode properties appear at moderate and high concentrations.

For $K_r=10^{-7}\,ms^{-1}$, the threshold is reduced to about 1 V at moderate N_{av} values between *c.* 3×10^{18} and $3\times10^{19}\,m^{-3}$. With further increase in concentration, the threshold is almost constant but finally decreases significantly reaching values as low as 0.5 V for $N_{av}\cong2\times10^{20}\,m^{-3}$.

For $K_r=10^{-6}\,ms^{-1}$, the threshold also has the reduced value of about 1 V for N_{av} in the range 10^{18}–$10^{19}\,m^{-3}$. At higher N_{av}, it increases again, however a tendency to decrease is seen at the largest ion concentration.

For $K_r=10^{-5}$ and $10^{-4}\,ms^{-1}$, the threshold has a minimum at $N_{av}\cong2\times10^{18}\,m^{-3}$. Enhancement of ion content gives rise to an increase of the threshold up to 3.3 V, indicating the approaching to the U_f value.

For $K_r=10^{-3}\,ms^{-1}$, the threshold weakly depends on concentration. Its magnitude remains close to U_f and varies between *c.* 3.5 and 3.3 V.

3.2. *Director distributions*

The various threshold voltages that occur at various average concentrations correspond to different forms of deformation. Four types of director distribution appearing at voltages slightly exceeding the threshold can be distinguished. Figure 2 shows representative examples obtained for $U=U_T+0.1$ V.

Type 1. Symmetric director distributions. These are similar to those obtained in insulating non-flexoelectric nematics and described by a nearly sinusoidal $\theta(\zeta)$ dependence with a maximum value at the centre of the layer. They appear if the electrodes are well conducting at any ion concentration ($K_r=10^{-3}\,ms^{-1}$, curve 1) as well as when the ion concentration is extremely low (e.g. $N_{av}<10^{17}\,m^{-3}$) for any of the considered electrode contacts (curve 2). The threshold voltage for this type of deformations is close to the U_f value.

Type 2. Asymmetric distributions without rapid change of orientation at the boundaries. The largest director deviation does not coincide with the mid-plane of the layer, nevertheless it takes place far from the boundary plates (curves 3, 4). This type of deformation occurs at moderate ion concentrations ($N_{av}\cong10^{18}$–$10^{19}\,m^{-3}$) and is most pronounced if the electrodes are poorly conducting. They are related to threshold voltages reduced to about 1 V.

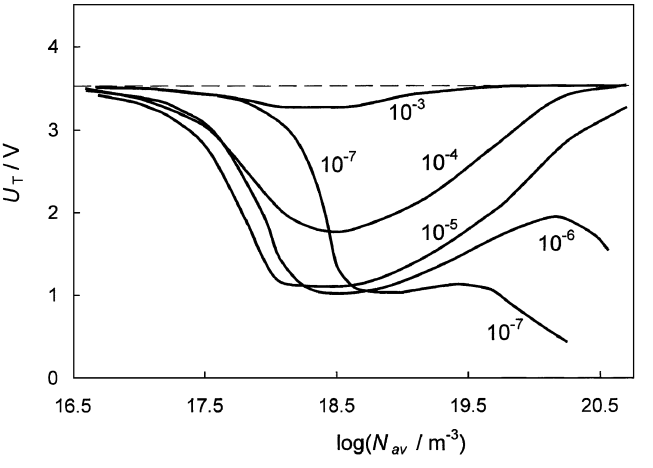

Figure 1. The threshold voltage U_T as a function of average ion concentration N_{av}, for five values of K_r indicated at each curve (in $m\,s^{-1}$). The dashed line represents the threshold $U_f=3.53$ V.

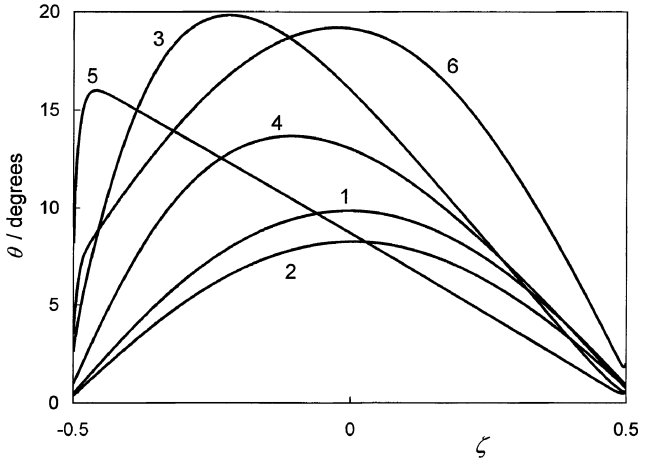

Figure 2. Director orientation angles θ as functions of the reduced coordinate ζ for $U=U_T+0.1$ V. See § 3 for values of parameters N_{av}, K_r and U.

Type 3. Highly asymmetric distributions. These result from rapid change of director orientation in the close neighbourhood of the negative electrode. The director orientation angle θ varies linearly with ζ between two significantly differing subsurface values (curve 5). This type of distribution occurs at high ion concentrations ($N_{av}>10^{20}\,m^{-3}$) if the electrode contacts are strongly blocking ($K_r=10^{-7}$–$10^{-6}\,ms^{-1}$) and is related to a very low threshold voltage (below 0.5 V).

Type 4. A distribution intermediate between types 2 and 3. The strongest director deviation takes place in the neighbourhood of the centre of the layer. The rapid change of orientation appears in the vicinity of the negative electrode. The corresponding thresholds exceeds 3 V. Distributions of this type occur at high ion concentrations ($N_{av}>10^{20}\,m^{-3}$) when the electrode contacts are intermediate between highly conducting and strongly blocking ($K_r=10^{-4}$–$10^{-5}\,ms^{-1}$). An example is given by curve 6.

3.3. *Ion concentration and electric field strength*

The director profiles distinguished above are due to different spatial variations of the electric field strength, which are connected with different distributions of ions. In general, the total number of positive ions is greater than the number of negative ions. The ions are gathered at the electrodes of opposite sign. The subelectrode concentrations are especially large if the electrodes are blocking.

3.3.1. Low ion concentrations ($N_{av}<10^{17}\,m^{-3}$). The number of positive ions is several times larger than the number of negative ions. However this effect, as well as variation of the ion concentrations with ζ (figure 3, curve 2), has only a minor influence on the electric field which remains practically uniform (figure 4, curve 2). The electric field strength value is very close to U/d. The resulting deformation is symmetrical.

3.3.2. Moderate ion concentrations ($N_{av}=10^{18}$–$10^{19}\,m^{-3}$). The variation of $N^{\pm}(\zeta)$ in the bulk is evident if the electrodes are poorly conducting. It is illustrated in figure 5 by curves 3 and 4. As a result, an electric field gradient arises, spreading over the whole thickness of the layer (figure 4, curve 4). In the strongly blocking case, the high concentrations at the electrodes give rise to enhanced subsurface electric fields (figure 4, curve 3). An asymmetrical deformation is induced in both cases. However the field gradient decreases and becomes negligible if the contacts are well conducting (figure 4, curve 1) which leads to symmetrical deformation. The number of positive ions is *c*. 1.1–2 times larger than the number of the negative ions.

3.3.3. High ion concentrations ($N_{av}>10^{20}\,m^{-3}$). In the case of blocking contacts, the ions are accumulated at the electrodes (figure 3, curves 5 and 6). They induce a high and non-uniform subsurface electric field (figure 4, curves 5 and 6). The electric field in the bulk is constant.

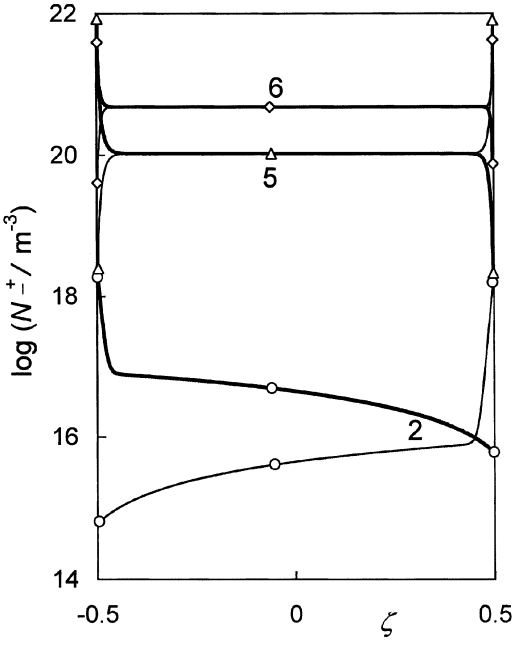

Figure 3. Low and high ion concentrations as functions of the reduced co-ordinate ζ for $U=U_T+0.1$ V; thin lines denote negative ions, thick lines denote positive ions. Rates of electrode processes K_r (in ms^{-1}) and voltages U (in volts) are as follows. 2: $K_r=10^{-6}$, $U=3.58$; 5: $K_r=10^{-7}$, $U=0.67$; 6: $K_r=10^{-5}$, $U=3.37$. Circles, triangles and diamonds identify concentration values at $\zeta=\pm 1/2$.

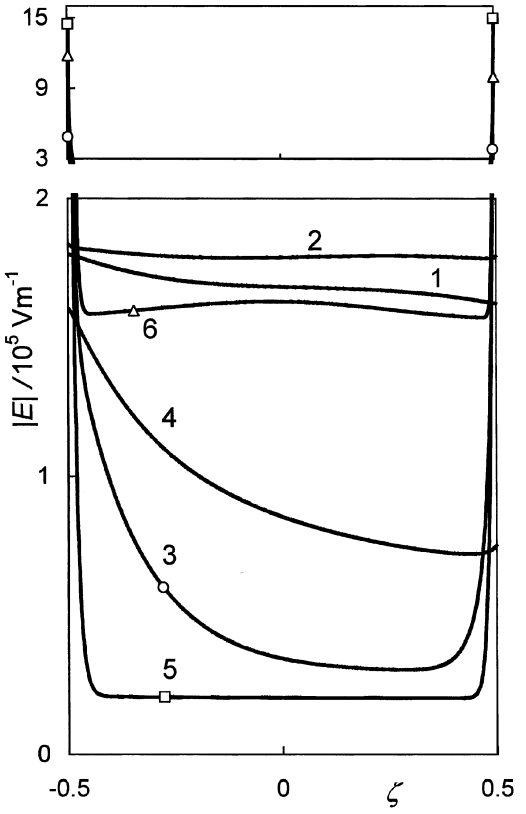

Figure 4. Electric field strength $|E|$ as a function of the reduced co-ordinate ζ for $U=U_T+0.1$ V. See §3 for values of parameters N_{av}, K_r and U. Circles, triangles and squares allow identification of values of $|E(\pm 1/2)|$.

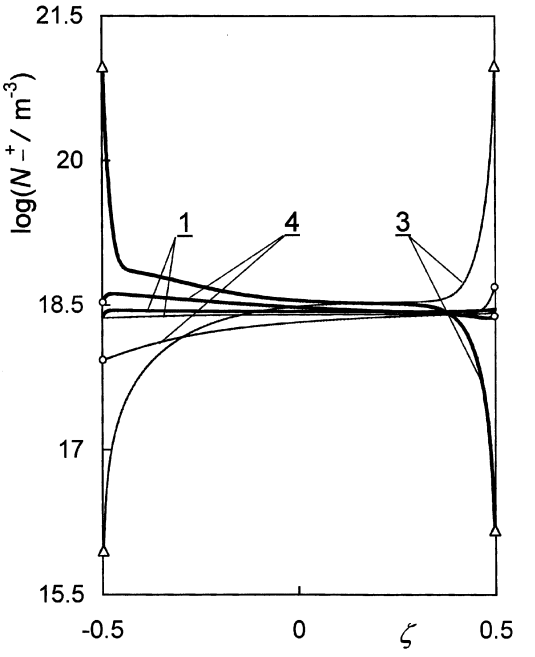

Figure 5. Moderate ion concentrations as functions of the reduced co-ordinate ζ for $U=U_T+0.1$ V; thin lines denote negative ions, thick lines denote positive ions. Rates of electrode processes K_r (in ms^{-1}) and voltages U (in volts) are as follows. 1: $K_r=10^{-3}$, $U=3.38$; 3: $K_r=10^{-7}$, $U=1.13$; 4: $K_r=10^{-4}$, $U=1.88$. Circles and triangles identify concentration values at $\zeta=\pm 1/2$.

Particularly high subsurface charges reduce the field strength in the bulk below the U/d value. The subsurface director orientation changes rapidly with ζ which is apparent at the negative electrode. The number of positive ions exceeds the number of the negative by *c.* 1%. In the case of well conducting contacts, the subelectrode ion concentrations slightly exceed the average value. The electric field strength is weakly affected by the space charges and remains practically uniform.

3.4. *Equal mobilities of positive and negative ions*

Additional calculations were performed for equal mobilities of negative and positive ions, $\mu^+=\mu^-$, with $\mu_{\|}{}^{\pm}/\mu_{\perp}{}^{\pm}=1.5$. The threshold voltages were determined for strongly blocking electrodes, $K_r=10^{-7}\,ms^{-1}$, for two values of mobility, the higher $\mu_{\perp}{}^{\pm}=1\times10^{-9}\,m^2V^{-1}s^{-1}$, and the lower $\mu_{\perp}{}^{\pm}=1\times10^{-10}\,m^2V^{-1}s^{-1}$. The thresholds are independent of the sign of the sum $e_{11}+e_{33}$. The results are presented in figure 6 by curves 1 and 2, respectively. They are compared with analogous

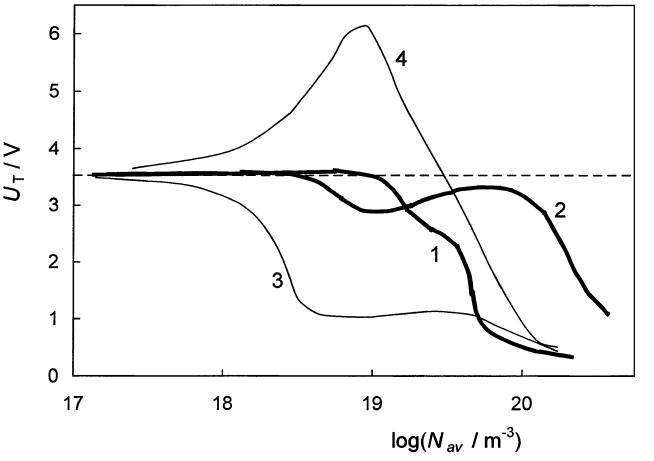

Figure 6. The threshold voltage U_T as a function of average ion concentration N_{av} for $K_r=10^{-7}\,ms^{-1}$. Thick lines denote equal mobilities (in $m^2V^{-1}s^{-1}$) of positive and negative ions, 1: $\mu_{\perp}{}^{\pm}=1\times10^{-9}$; 2: $\mu_{\perp}{}^{\pm}=1\times10^{-10}$. Thin lines denote unequal mobilities, $\mu_{\perp}{}^{-}=1\times10^{-9}$, $\mu_{\perp}{}^{+}=1\times10^{-10}$; 3: $e_{11}+e_{33}>0$; 4: $e_{11}+e_{33}<0$. The dashed line represents the threshold $U_f=3.53$ V.

functions found for unequal mobilities. Curve 3 is repeated from figure 1, whereas curve 4 is obtained from our calculations performed for $e_{11}+e_{33}<0$ [7]. For extreme ion concentrations, the threshold voltages have similar values in all the cases considered. Namely, for low ion contents, the thresholds are close to U_f, and for high ion concentration they tend to a very low value of *c.* 0.5 V. One can distinguish moderate ion concentrations, for which the thresholds differ from the U_T values found for the $\mu^+ \ll \mu^-$ case. For higher mobility, the range of moderate ion concentrations extends from 1×10^{19} to $5\times10^{19}\,m^{-3}$. The threshold decreases monotonically from *c.* 3.5 to *c.* 2.5 V. For lower mobility, such a range lies between 5×10^{18} and $5\times10^{19}\,m^{-3}$. The $U_T(N_{av})$ function exhibits a minimum of *c.* 3 V followed by an increase to a maximum of 3.3 V, which precedes a steep decrease occurring at high N_{av}.

The director distributions have the same forms as described in § 3.2. For low ion contents, the director profiles are symmetrical (similar to that shown in figure 2 by curve 2) and for high ion concentrations they possess evident linear part (such as the profile presented by curve 5 in figure 2). For moderate concentrations, characteristic asymmetric director distributions occur, similar to those shown in figure 2 by curves 3 and 4. Profiles of type 4 (figure 2, curve 6) have also been observed for the lower mobility.

The electric field distributions are symmetrical (figure 7). Therefore at low and high ion concentrations, the electric field plays a similar role to the field arising in the case of unequal mobilities. For moderate ion contents, the symmetrical $E(\zeta)$ distributions are essentially different from the case of unequal mobilities. In particular, the positive and negative electric field gradients exist in the negative and in the positive half of the layer, respectively, instead of the positive gradient spreading over the whole layer.

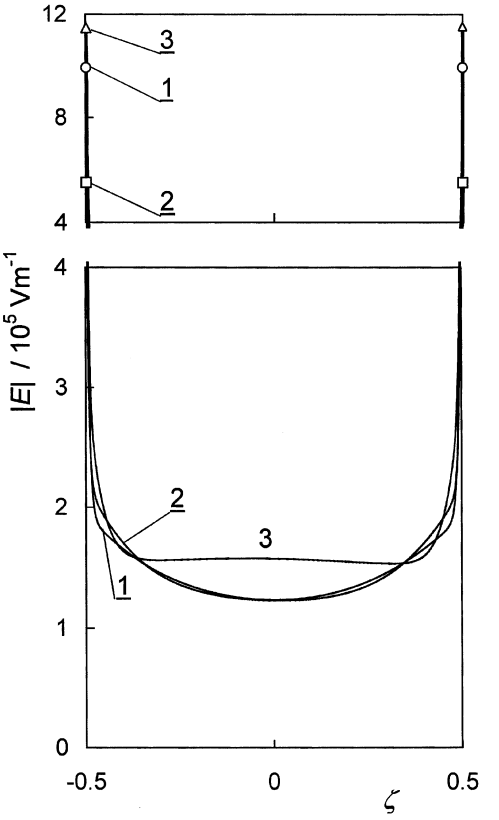

Figure 7. Electric field strength $|E|$ as a function of the reduced co-ordinate ζ for $K_r=10^{-7}\,ms^{-1}$ and equal mobilities (in $m^2\,V^{-1}\,s^{-1}$) of positive and negative ions, 1: $\mu_\perp{}^+=1\times10^{-9}$; 2 and 3: $\mu_\perp{}^+=1\times10^{-10}$. Average ion concentrations N_{av} (in m^{-3}) and voltages U (in volts, $U=U_T+0.1$ V) are as follows: 1: $N_{av}=1.7\times10^{19}$, $U=3.02$; 2: $N_{av}=1.0\times10^{19}$, $U=2.99$; 3: $N_{av}=5.1\times10^{19}$, $U=3.42$. Circles, triangles and squares permit identification of the values of $|E(\pm1/2)|$.

4. Discussion

Deformations are caused by torques of twofold nature: (i) dielectric, expressed by the third term of equation (5), and (ii) flexoelectric, given by the fourth term of equation (5) and by the first terms of equations (7). The main results presented above were obtained for a homeotropic layer containing a nematic with $\Delta\varepsilon<0$, $e_{11}+e_{33}>0$ and $\mu^+\ll\mu^-$. The torque due to the negative dielectric anisotropy is destabilizing. The flexoelectric torques acting at the boundary surfaces are proportional to the electric field strength, $E(\pm1/2)$. According to the positive sum of flexoelectric coefficients, they are destabilizing at $\zeta=1/2$ and stabilizing at $\zeta=-1/2$. The bulk flexoelectric torque depends on the electric field gradient and favours the deformations if $d^2V/d\zeta^2<0$ and damps them in the opposite case. All these torques determine the threshold voltage U_T. In the following, the results will be discussed separately for high, low and moderate average ion concentrations.

4.1. *High ion concentrations ($N_{av}>10^{20}\,m^{-3}$)*

In the case of strongly blocking electrodes ($K_r=10^{-7}\,ms^{-1}$), the large field gradient in the vicinity of $\zeta=-1/2$, $d^2V/d\zeta^2<0$, gives rise to significant deformations arising above a very small threshold voltage of *c.* 0.5 V. The surface flexoelectric torque at $\zeta=-1/2$ is, however, stabilizing and therefore the angle $\theta(-1/2)$ is smaller than in the neighbourhood of negative electrode. In consequence, a rapid change of director orientation occurs in the subsurface region. The bulk flexoelectric torque created by the field gradient $d^2V/d\zeta^2>0$ in the vicinity of $\zeta=1/2$ has a stabilizing effect which overwhelms the destabilizing surface torque due

to $E(1/2)$. The angle $\theta(1/2)$ is therefore close to zero. The electric field strength in the bulk is rather low, $E<U/d$, so the dielectric torque does not give a noticeable contribution. The resulting director distribution is shown by curve 5 in figure 2. The results are qualitatively the same, both for equal and unequal mobilities of positive and negative ions.

If the blocking character of the electrodes is somewhat less pronounced ($K_r=10^{-5}\,ms^{-1}$), the ion accumulation at the electrodes is also less intensive. The destabilizing flexoelectric torques mentioned above are weaker, and the voltage necessary for deformation is higher than previously. The threshold voltage rises to *c*. 3.3 V, which is close to U_f. The electric field in the bulk is high enough to create the dielectric torque leading to deformation illustrated by curve 6 in figure 2.

The more conducting are the electrode contacts, the more symmetrical becomes the deformation. If the electrodes are well conducting, the electric field is constant throughout the layer, $d^2V/d\zeta^2\approx 0$. The only torque in the bulk is of dielectric nature; it prevails over the weak surface flexoelectric torques and leads to symmetrical deformation appearing at $U_T\approx U_f$, (figure 2, curve 1).

4.2. *Low ion concentrations ($N_{av}<10^{17}\,m^{-3}$)*

In a layer with low ion contents, there is no reason for substantial field gradients. The dielectric torque in the bulk induces symmetrical deformation at $U\approx U_f$ in the same way as mentioned above (figure 2, curve 2). The relationship between the mobilities of positive and negative ions is of no importance.

4.3. *Moderate ion concentrations ($N_{av}=10^{18}$–$10^{19}\,m^{-3}$)*

The surface fields $E(\pm 1/2)$, as well as the subsurface gradients, are smaller than in the previous case. However the ion distributions give rise to a destabilizing field gradient $d^2V/d\zeta^2<0$ spreading over the layer. Although relatively small, it reaches a value already sufficient for deformation at $U=1$ V (for $K_r=10^{-7}-10^{-6}\,ms^{-1}$). In this way, the threshold voltage is reduced markedly below the U_f value. The reduction weakens with increase of K_r, e.g. $U_T\approx 2$ V for $K_r=10^{-4}\,ms^{-1}$. Director profiles have a distinctive asymmetric form (curves 3 and 4 in figure 2).

The electric field gradient in the bulk results from asymmetric ion distributions which is essential at moderate N_{av} (curves 3 and 4 in figure 5). The asymmetry has its origin in the difference between mobilities of positive and negative ions, $\mu^+\ll\mu^-$. The role of mobility values is demonstrated by additional calculations performed with equal mobilities, $\mu^+=\mu^-$, for blocking electrodes, i.e. for $K_r=10^{-7}\,ms^{-1}$.

The gradients due to symmetrical electric field distributions have opposite signs in the two halves of the layer. Their destabilizing and stabilizing actions are partially compensated. The reduction of the threshold is therefore weaker than in the case of $\mu^+\ll\mu^-$ and the U_T values do not decrease below *c*. 3 V. The deformations have an asymmetric form.

The data presented above are consistent with our earlier results. The gradient term which appears if $\mu^+\ll\mu^-$ is stabilizing if $e_{11}+e_{33}<0$ and enhances the threshold. This effect was predicted by our earlier calculations concerning the nematic with a negative sum of the flexoelectric coefficients [7]. The corresponding $U_T(N_{av})$ functions are plotted for comparison in figure 6.

The behaviour of the layer predicted by our numerical calculations indicate that analysis of experimental data concerning elastic deformations induced by a d.c. electric field should take into account the flexoelectric properties of the nematic liquid crystal, the ion contents and their mobilities, and the properties of the electrodes. The effects due to space charges can be ignored only if the ion concentrations are very low. Nevertheless, the flexoelectric properties should be considered also in this case, unless the surface anchoring strength is very large. In the case of well conducting electrodes, the results can be qualitatively similar to the insulating case but they may differ quantitatively. The application of theoretical predictions derived for insulating nematics to the interpretation of data obtained for a conducting nematic confined between blocking electrodes may lead to false conclusions. The significance of the effects described in this paper could be estimated by comparison of the results obtained from experiments performed in a d.c. electric field and in a magnetic field.

Summarizing, our main conclusions are: (1) low ion contents or conducting electrodes result in symmetrical deformations arising at threshold voltages close to U_f; (2) blocking electrodes at high ion concentrations give very low thresholds; (3) mobility values play an important role if the ion concentration is moderate; (4) the threshold may be markedly enhanced or reduced, depending on the subtle relationships between μ^+ and μ^- and on the sign of the sum $e_{11}+e_{33}$.

References

[1] L.M. Blinov, V.G. Chigrinov. *Electro-optic Effects in Liquid Crystal Materials*. (Springer Verlag, New York) (1993).

[2] M. Felczak, G. Derfel. *Liq. Cryst.*, **30**, 739 (2003).

[3] M. Felczak, G. Derfel. *Proc. SPIE*, **5565**, 191 (2004).
[4] G. Briere, F. Gaspard, R. Herino. *J. chim. Phys.*, **68**, 845 (1971).
[5] H. Naito, M. Okuda, A. Sugimura. *Phys. Rev. A*, **44**, R3434 (1991).
[6] M.Y. Jin, J.-J. Kim. *J. Phys. condens. Matter*, **13**, 4435 (2001).
[7] G. Derfel, M. Buczkowska, *Liq. Cryst.* (in press).
[8] G. Derfel, A. Lipiński. *Mol. Cryst. liq. Cryst.*, **55**, 89 (1979).
[9] S. Naemura, Y. Nakazono, K. Nishikawa, A. Sawada, P. Kirsch, M. Bremer, K. Tarumi. *Mat. Res. Soc. Symp., Proc.*, **508**, 235 (1998).
[10] H. de Vleeschouwer, A. Verschueren, F. Bougriona, R. van Asselt, E. Alexander, S. Vermael, K. Neyts, H. Pauwels. *Jpn. J. appl. Phys.*, **40**, 3272 (2001).
[11] D. Potter. *Computational Physics*. (John Wiley, London) (1973).
[12] A. Derzhanski, A.G. Petrov, M.D. Mitov. *J. Phys. (Paris)*, **39**, 273 (1978).